Cooperative Uplink NOMA in D2D Communications

Athanasios P. Chrysologou, Student Member, IEEE, Nestor D. Chatzidiamantis, Member, IEEE, and George K. Karagiannidis, Fellow, IEEE

***Abstract*—In this work, we propose and investigate a novel hybrid cellular and bidirectional device-to-device (D2D) transmission scheme that exploits cooperative non-orthogonal multiple access (termed as BD2D-CNOMA). In BD2D-CNOMA, two far users can transmit their messages to the base station (BS) via a relaying node, while simultaneously they exchange D2D messages. Analytical expressions for the ergodic capacity, ergodic sum capacity (ESC) and outage probability of all data streams are derived under both perfect and imperfect successive interference cancellation (SIC). Furthermore, it is proved that ESC under perfect SIC scales as $\frac{2}{3}\log_2\rho$ as transmit signal-to-noise ratio ρ increases. Simulation results validate the accuracy of the presented analysis, illustrate the superiority of BD2D-CNOMA over conventional benchmarks under perfect SIC and provide useful insights for the case of imperfect SIC.**

***Index Terms*—Bidirectional device-to-device (D2D), non orthogonal multiple access (NOMA), successive interference cancellation (SIC), ergodic rate, outage probability.**

I. Introduction

THE exponential growth of data traffic which is required to be managed by the next generation networks has led to the need of high spectral efficiency (SE). In this direction, the investigation of non-orthogonal multiple access (NOMA) was the main scope of many research efforts. In NOMA, the same orthogonal resource is shared by multiple users by assigning them different power levels. Thus, the network capacity and SE can be increased [1]. However, cell-edge users still show poor performance. In this direction, cooperative NOMA (CNOMA) was suggested [2], according to which a relaying node assists the communication between base station (BS) and far users. Furthermore, another promising key technology able to boost next generation networks' SE is device-to-device (D2D) communications [3], which allow nearby devices to communicate directly with each other and not via a BS.

Since both CNOMA and D2D are significant SE enhancing technologies, the combination of CNOMA and D2D has been considered in a few works. In [4], a D2D-aided full-duplex CNOMA scheme, where the NOMA-strong user helps the NOMA-weak user, was proposed and investigated, while in [5], a successive user relaying approach was used in order to improve the SE of a CNOMA system. Furthermore, in [6], a novel framework on the D2D-enabled heterogeneous networks with NOMA, which improved system's SE, was presented. In [7], it was proved that when the relaying node shares its own message with the cell-center user, then the resultant D2D-aided coordinated direct and relay NOMA-based scheme (CDRT-NOMA) can improve its ergodic sum capacity (ESC) performance. In [8], the scaling of the ESC in a cooperative downlink NOMA setup was investigated, while in [9], a joint downlink-uplink CDRT-NOMA scheme that uses D2D transmissions to further improve its ESC, was proposed. Moreover, in [10], a D2D-aided uplink NOMA scheme with one far and two near users that transmit cellular messages and exchange one-directional D2D messages, was investigated.

The authors are with the Department of Electrical and Computer Engineering, Aristotle University of Thessaloniki, 54124 Thessaloniki, (e-mails: chrysolog@ece.auth.gr, nestoras@auth.gr, geokarag@auth.gr).

Although the existing literature has extensively investigated D2D-assisted NOMA networks, where D2D links act as relays for cellular messages [2], [4]–[6], [9], the efficient integration of (C-)NOMA and bidirectional D2D, in cases where D2D links allow users to share traffic generated by themselves, still remains relatively unexplored [11]. Hence, in this work, a hybrid cellular and bidirectional D2D communication network is proposed, where both cellular and bidirectional D2D communications in the same frequency, occur. In such a network, simultaneously with cellular communication, numerous applications can be supported via the bidirectional D2D communication, such as peer-to-peer content sharing, multiplayer gaming, social networking, etc [12].

Furthermore, compared to [4]–[10], where only perfect successive interference cancellation (pSIC) is considered, in this work the impact of imperfect SIC (impSIC) is investigated.

Hence, the contribution of our work can be summarized as follows. A novel 3-phase half-duplex transmission scheme (termed as BD2D-CNOMA) for the efficient hybrid cellular and bidirectional D2D communication in a network with two far users assisted by a relaying node, is proposed. System's performance is investigated, under both pSIC and impSIC, by providing closed-form expressions for the outage probabilities (OPs) and ergodic capacities (ECs) of all data streams. Also, it is proved that, under pSIC, ESC scales as $\frac{2}{3}\log_2\rho$ as transmit signal-to-noise ratio ρ increases and the superiority of the proposed scheme over conventional benchmarks is validated via both numerical and simulation results.

II. System model and protocol description

As depicted in Fig. 1, a cooperative NOMA system is considered, where two far users, U_1 and U_2, communicate not only with a BS, but also with each other by exchanging D2D messages in order to complete a bidirectional communication. The direct links between U_1, U_2 and the BS are neglected due to heavy shadow conditions [9] and, regarding the long distance, a decode-and-forward (DF) relaying node is used for aiding the transmissions from U_1, U_2 to the BS. Furthermore, all nodes are assumed to be equipped with a single antenna and operate in the half-duplex mode, while both pSIC and the practical case of impSIC are considered.

The channels from U_1 and U_2 to the relay and from the relay to the BS are denoted by h_{1r}, h_{2r} and h_{rb} respectively.

This article has been accepted for publication in IEEE Communications Letters. This is the author's version which has not been fully edited and content may change prior to final publication. Citation information: DOI 10.1109/LCOMM.2022.3199083

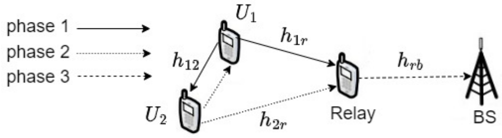

Fig. 1: System model

Moreover, the channel between U_1 and U_2 is considered reciprocal and is denoted by h_{12}. All the wireless channels undergo independent block-flat Rayleigh fading plus additive white Gaussian noise (AWGN) with zero mean and variance N_o. The complex channel coefficient is denoted by $h_{i,j} \sim CN(0, \lambda_{i,j} = d_{i,j}^{-\epsilon})$ with zero mean and variance $\lambda_{i,j}$, where ϵ is the path loss exponent and $d_{i,j}$ is the distance between two nodes i, j. Hence, $|h_{i,j}|^2$ follows exponential distribution with mean value $\lambda_{i,j}$. The distances between the nodes are assumed to be known from network's nodes and $d_{12} = d_{21} < d_{1r} < d_{2r}$ is considered. This is, also, in agreement with the short range links that D2D communications require [3].

The transmission protocol is divided into three equal consecutive phases and each phase requires one time slot. In Phase-1, U_1 transmits a composite signal $x_{t_1} = \sqrt{a_1 P_u} x_1 + \sqrt{a_2 P_u} x_{12}$, where message x_1 is the uplink message of U_1 and x_{12} is a D2D message from U_1 to U_2, P_u is users' transmit power and a_1, a_2 denote the power allocation coefficients, such that $a_1 + a_2 = 1$. We assume $a_1 > a_2$ since $d_{12} < d_{1r}$ [1]. Hence, in BD2D-CNOMA, it is proposed that U_1 can complete a cellular transmission to BS (via a DF relay) and at the same time share data with cellular user U_2. According to the decoding principle in NOMA, U_2 must firstly decode x_1 and then, via SIC, to decode x_{12}. More specifically, the received SINRs at U_2 are the following

$$\gamma_{x_1,2} = \frac{a_1 |h_{12}|^2 \rho_u}{a_2 |h_{12}|^2 \rho_u + 1}, \quad \gamma_{x_{12}} = \frac{a_2 |h_{12}|^2 \rho_u}{a_1 |g_{12}|^2 \rho_u + 1}, \tag{1}$$

where $\rho_u = \frac{P_u}{No}$ is users' transmit SNR and $g_{12} \sim CN(0, k_{12}\lambda_{12})$, where k_{12} denotes the level of residual interference due to impSIC [11], with $0 \leq k_{12} \leq 1$. Cases $k_{12} = 0$, $k_{12} = 1$ denote pSIC and no SIC, respectively. Similarly, the SINR at the relay to decode x_1, is expressed as

$$\gamma_{x_1,r} = \frac{a_1 |h_{1r}|^2 \rho_u}{a_2 |h_{1r}|^2 \rho_u + 1}. \tag{2}$$

In Phase-2, U_2 transmits a composite signal $x_{t_2} = \sqrt{b_1 P_u} x_2 + \sqrt{b_2 P_u} x_{21}$, where message x_2 is the uplink message of U_2, x_{21} is a D2D message from U_2 to U_1 and b_1, b_2 denote the power allocation coefficients, such that $b_1 + b_2 = 1$ and $b_1 > b_2$ since $d_{21} < d_{2r}$. In this phase, the bidirectional communication between U_1 and U_2 is completed. Similarly with phase-1, the received SINRs at U_1 and relay are the following

$$\gamma_{x_2,1} = \frac{b_1 |h_{12}|^2 \rho_u}{b_2 |h_{12}|^2 \rho_u + 1}, \quad \gamma_{x_{21}} = \frac{b_2 |h_{12}|^2 \rho_u}{b_1 |g_{21}|^2 \rho_u + 1}, \tag{3}$$

$$\gamma_{x_2,r} = \frac{b_1 |h_{2r}|^2 \rho_u}{b_2 |h_{2r}|^2 \rho_u + 1}, \tag{4}$$

where $g_{21} \sim CN(0, k_{21}\lambda_{12})$ with k_{21} denoting the impact of impSIC at U_1.

In Phase-3, relay forwards users' uplink messages to BS. The message that is forwarded depends on which message(s) were successfully decoded at the relay in the previous two phases. More specifically, there are four different cases: I) relay succeeded in decoding both x_1 in phase-1 and x_2 in phase-2 and, thus, the message that forwards to BS is $x_r^I = \sqrt{c_1 P_r} x_1 + \sqrt{c_2 P_r} x_2$, where P_r is relay's transmit power and c_1, c_2 denote the power allocation coefficients, such that $c_1 + c_2 = 1$, II) relay succeeded in decoding x_1 in phase-1, but wasn't able to decode x_2 in phase-2, and thus, forwards $x_r^{II} = \sqrt{P_r} x_1$, III) relay did not succeed in decoding x_1 in phase-1, but was able to decode x_2 in phase-2, and thus, forwards $x_r^{III} = \sqrt{P_r} x_2$, and IV) relay didn't decode any of the messages and, hence, remains silent in phase-3.

For case (I), without loss of generality, we assume that $c_1 > c_2$[1]. and thus, the decoding order at BS starts with x_1. Hence, the received SINRs at BS for case (I) are the following:

$$\gamma_{x_1,b}^I = \frac{a_1 |h_{rb}|^2 \rho_r}{a_2 |h_{rb}|^2 \rho_r + 1}, \quad \gamma_{x_2,b}^I = \frac{a_2 |h_{rb}|^2 \rho_r}{a_1 |g_{rb}|^2 \rho_r + 1}, \tag{5}$$

where $\rho_r = \frac{P_r}{N_o}$ and $g_{rb} \sim CN(0, k_{rb}\lambda_{rb})$ models the residual interference at BS due to impSIC.

On the other hand, in case (II) only x_1 is forwarded to the BS, while in case (III) only x_2 is forwarded to the BS. Hence,

$$\gamma_{x_1,b}^{II} = |h_{rb}|^2 \rho_r, \quad \gamma_{x_2,b}^{III} = |h_{rb}|^2 \rho_r. \tag{6}$$

III. Outage Probability Analysis

When users transmit at constant rates $\bar{R}_m$, where $m \in \{x_1, x_2, x_{12}, x_{21}\}$, OP is a significant performance criterion. An outage occurs when SINR falls below a threshold, which can be defined as $\gamma_m^{thr} = 2^{3\bar{R}_m} - 1$.

Next, closed-form expressions for the OP of x_1, x_2, x_{12} and x_{21} are derived. For x_1, in order to avoid outage, it is necessary that x_1 is decoded at both relay and BS. Hence,

$$P_{x_1}^{out} = 1 - \Big(\Pr(\gamma_{x_1,r} \geq \gamma_{x_1}^{thr}) \Pr(\gamma_{x_2,r} \geq \gamma_{x_2}^{thr}) \Pr(\gamma_{x_1,b}^I \geq \gamma_{x_1}^{thr}) + \Pr(\gamma_{x_1,r} \geq \gamma_{x_1}^{thr}) \Pr(\gamma_{x_2,r} < \gamma_{x_2}^{thr}) \Pr(\gamma_{x_1,b}^{II} \geq \gamma_{x_1}^{thr}) \Big). \tag{7}$$

All SINR terms that appear in (7) can be written as $Y = \frac{aX}{bX+1}$ where a, b are positive constants and X is exponentially distributed with mean λ_x. It can be easily shown that the cumulative distribution function (CDF) of Y is given as:

$$F_Y(y) = \begin{cases} 1 - e^{-\frac{1}{\lambda_x}\frac{y}{a-by}}, & y < \frac{a}{b} \\ 1, & y \geq \frac{a}{b}. \end{cases} \tag{8}$$

Hence, after some basic algebraic manipulations we get

$$P_{x_1}^{out} = \begin{cases} 1 - e^{-M(a_1,\lambda_{1r},\rho_u,\gamma_{x_1}^{thr})} \Big(e^{-\frac{\gamma_{x_1}^{thr}}{\lambda_{rb}\rho_r}} - e^{-M(b_1,\lambda_{2r},\rho_u,\gamma_{x_2}^{thr})} \\ \big(e^{-\frac{\gamma_{x_1}^{thr}}{\lambda_{rb}\rho_r}} - e^{-M(a_1,\lambda_{rb},\rho_r,\gamma_{x_1}^{thr})}\big)\Big), \gamma_{x_1}^{thr} < \frac{a_1}{a_2}, \gamma_{x_2}^{thr} < \frac{b_1}{b_2} \\ 1 - e^{-\frac{\gamma_{x_1}^{thr}}{\lambda_{rb}\rho_r} - M(a_1,\lambda_{1r},\rho_u,\gamma_{x_1}^{thr})}, \gamma_{x_1}^{thr} < \frac{a_1}{a_2}, \gamma_{x_2}^{thr} \geq \frac{b_1}{b_2} \\ 1, \quad \text{elsewhere.} \end{cases} \tag{9}$$

[1]Similarly with [7], for mathematical tractability, we assume that $c_1 = a_1$ and, thus, $c_2 = a_2$. However, the analysis can be straightforwardly extended for arbitrary c_1, c_2

where $M(v,\lambda,p,q)=\frac{q}{v\lambda p-(1-v)\lambda pq}$. It is noted that x_1's OP is not affected from impSIC since, in all phases, x_1's message is decoded first.

Similarly with x_1, in order to avoid outage, x_2 must be decoded at both relay and BS. Hence,

$$P^{out}_{x_2}=1-\Big(\Pr(\gamma_{x_2,r}\geq\gamma^{thr}_{x_2})\Pr(\gamma_{x_1,r}<\gamma^{thr}_{x_1})\times\Pr(\gamma^{III}_{x_2,b}\geq\gamma^{thr}_{x_2})+\Pr(\gamma_{x_2,r}\geq\gamma^{thr}_{x_2})P(\gamma_{x_1,r}\geq\gamma^{thr}_{x_1})\times\Pr(\gamma^{I}_{x_1,b}\geq\gamma^{thr}_{x_1},\gamma^{I}_{x_2,b}\geq\gamma^{thr}_{x_2})\Big). \tag{10}$$

Except $\Pr(\gamma^{I}_{x_1,b}\geq\gamma^{thr}_{x_1},\gamma^{I}_{x_2,b}\geq\gamma^{thr}_{x_2})$, all the other probabilities of (10) can be straightforwardly calculated through (8). Furthermore, it holds

$$\begin{aligned}&\Pr(\gamma^{I}_{x_1,b}\geq\gamma^{thr}_{x_1},\gamma^{I}_{x_2,b}\geq\gamma^{thr}_{x_2})\\&=\Pr(\frac{a_1|h_{rb}|^2\rho_r}{a_2|h_{rb}|^2\rho_r+1}\geq\gamma^{thr}_{x_1},\frac{a_2|h_{rb}|^2\rho_r}{a_1|g_{rb}|^2\rho_r+1}\geq\gamma^{thr}_{x_2})\\&=\begin{cases}\Pr(|h_{rb}|^2\geq A,|h_{rb}|^2\geq B), & \gamma^{thr}_{x_1}<\frac{a_1}{a_2}\\0, & \gamma^{thr}_{x_1}\geq\frac{a_1}{a_2}\end{cases}\end{aligned} \tag{11}$$

where $A=\frac{\gamma^{thr}_{x_1}}{a_1\rho_r-a_2\rho_r\gamma^{thr}_{x_1}}$, $B=\frac{\gamma^{thr}_{x_2}a_1|g_{rb}|^2\rho_r+\gamma^{thr}_{x_2}}{a_2\rho_r}$. It can be shown that $A\geq B$ holds when $|g_{rb}|^2\leq\frac{a_2\rho_rA-\gamma^{thr}_{x_2}}{a_1\gamma^{thr}_{x_2}\rho_r}\triangleq C$, whereas $A<B$ holds when $|g_{rb}|^2>C$. Hence, (11) becomes

$$\begin{aligned}&\Pr(\gamma^{I}_{x_1,b}\geq\gamma^{thr}_{x_1},\gamma^{I}_{x_2,b}\geq\gamma^{thr}_{x_2})\\&=\begin{cases}\big(1-F_{|h_{rb}|^2}(A)\big)F_{|g_{rb}|^2}(C)\\+\int_C^\infty(1-F_{|h_{rb}|^2}(B_y))f_{|g_{rb}|^2}(y)\mathrm{d}y, & \gamma^{thr}_{x_1}<\frac{a_1}{a_2},\ C>0\\\int_0^\infty(1-F_{|h_{rb}|^2}(B_y))f_{|g_{rb}|^2}(y)\mathrm{d}y, & \gamma^{thr}_{x_1}<\frac{a_1}{a_2},\ C<0\\0, & \gamma^{thr}_{x_1}\geq\frac{a_1}{a_2}\end{cases}\\&=\begin{cases}e^{-\frac{A}{\lambda_{rb}}}(1-e^{-\frac{C}{k_{rb}\lambda_{rb}}})+\frac{1}{Dk_{rb}\lambda_{rb}}\\\times e^{-\frac{\gamma^{thr}_{x_2}}{a_2\rho_r\lambda_{rb}}-DC}, & \gamma^{thr}_{x_1}<\frac{a_1}{a_2},\ C>0\\\frac{1}{Dk_{rb}\lambda_{rb}}e^{-\frac{\gamma^{thr}_{x_2}}{a_2\rho_r\lambda_{rb}}}, & \gamma^{thr}_{x_1}<\frac{a_1}{a_2},\ C<0\\0, & \gamma^{thr}_{x_1}\geq\frac{a_1}{a_2}\end{cases}\end{aligned} \tag{12}$$

where $B_y=\frac{\gamma^{thr}_{x_2}a_1y\rho_r+\gamma^{thr}_{x_2}}{a_2\rho_r}$, $D=\frac{\lambda^2_{rb}a_2\rho_rk_{rb}}{\gamma^{thr}_{x_2}a_1\rho_rk_{rb}\lambda_{rb}+\lambda_{rb}a_2\rho_r}$ and $F(\cdot)$, $f(\cdot)$ denote the CDF and probability density function (PDF), respectively. By combining all the above, we get $P^{out}_{x_2}$ which is given via (13) shown at the top of the next page.

It is noted that for the extraction of x_2's OP under pSIC, (10) can be used as soon as $\Pr(\gamma^{I}_{x_1,b}\geq\gamma^{thr}_{x_1},\gamma^{I}_{x_2,b}\geq\gamma^{thr}_{x_2})$ is appropriately updated. More specifically, under pSIC, it holds

$$\begin{aligned}&\Pr(\gamma^{I}_{x_1,b}\geq\gamma^{thr}_{x_1},\gamma^{I}_{x_2,b}\geq\gamma^{thr}_{x_2})\\&=\Pr(\frac{a_1|h_{rb}|^2\rho_r}{a_2|h_{rb}|^2\rho_r+1}\geq\gamma^{thr}_{x_1},a_2|h_{rb}|^2\rho_r\geq\gamma^{thr}_{x_2})\\&\overset{(a)}{=}\begin{cases}e^{-\frac{\phi}{\lambda_{rb}}}, & \gamma^{thr}_{x_1}<\frac{a_1}{a_2}\\0, & \gamma^{thr}_{x_1}\geq\frac{a_1}{a_2}\end{cases}\end{aligned} \tag{14}$$

where (a) follows from (8) and $\phi=\max(\frac{\gamma^{thr}_{x_1}}{a_1\rho_r-a_2\rho_r\gamma^{thr}_{x_1}},\frac{\gamma^{thr}_{x_2}}{a_2\rho_r})$. By invoking (14) in (10), we get

$$P^{p}_{x_2}=\begin{cases}1-(e^{-\frac{\gamma^{thr}_{x_2}}{\lambda_{rb}\rho_r}}-e^{-M(a_1,\lambda_{1r},\rho_u,\gamma^{thr}_{x_1})}(e^{-\frac{\gamma^{thr}_{x_2}}{\lambda_{rb}\rho_r}}-e^{-\frac{\phi}{\lambda_{rb}}}))\\e^{-M(b_1,\lambda_{2r},\rho_u,\gamma^{thr}_{x_2})}, \gamma^{thr}_{x_1}<\frac{a_1}{a_2},\gamma^{thr}_{x_2}<\frac{b_1}{b_2}\\1-e^{-\frac{\gamma^{thr}_{x_2}}{\lambda_{rb}\rho_r}-M(b_1,\lambda_{2r},\rho_u,\gamma^{thr}_{x_2})}, \gamma^{thr}_{x_1}\geq\frac{a_1}{a_2},\gamma^{thr}_{x_2}<\frac{b_1}{b_2}\\1,\text{elsewhere.}\end{cases} \tag{15}$$

In order to avoid outage for x_{12}, in phase-1 U_2 must firstly succeed in decoding x_1 and then be able to decode x_{12} through SIC, thus, $P^{out}_{x_{12}}=1-\Pr(\gamma_{x_1,2}\geq\gamma^{thr}_{x_1},\gamma_{x_{12}}\geq\gamma^{thr}_{x_{12}})$. Following similar lines with the extraction of (12), it holds

$$P^{out}_{x_{12}}=\begin{cases}1-e^{-\frac{\tilde{A}}{\lambda_{12}}}(1-e^{-\frac{\tilde{C}}{k_{12}\lambda_{12}}})+\frac{1}{\tilde{D}k_{12}\lambda_{12}}\\\times e^{-\frac{\gamma^{thr}_{x_{12}}}{a_2\rho_u\lambda_{12}}-\tilde{D}\tilde{C}}, & \gamma^{thr}_{x_{12}}<\frac{a_1}{a_2},\tilde{C}>0\\1-\frac{1}{\tilde{D}k_{12}\lambda_{12}}e^{-\frac{\gamma^{thr}_{x_{12}}}{a_2\rho_u\lambda_{12}}}, & \gamma^{thr}_{x_{12}}<\frac{a_1}{a_2},\tilde{C}<0\\1, & \gamma^{thr}_{x_{12}}\geq\frac{a_1}{a_2}\end{cases} \tag{16}$$

where $\tilde{A}=\frac{\gamma^{thr}_{x_1}}{a_1\rho_u-a_2\rho_u\gamma^{thr}_{x_1}}$, $\tilde{C}=\frac{a_2\rho_u\tilde{A}-\gamma^{thr}_{x_{12}}}{a_1\gamma^{thr}_{x_{12}}\rho_u}$ and $\tilde{D}=\frac{\lambda^2_{12}a_2\rho_uk_{12}}{a_1\gamma^{thr}_{x_{12}}\rho_uk_{12}\lambda_{12}+\lambda_{12}a_2\rho_u}$.

On the other hand, if pSIC is assumed, then

$$\begin{aligned}P^{p}_{x_{12}}&=1-\Pr(\frac{a_1|h_{12}|^2\rho_u}{a_2|h_{12}|^2\rho_u+1}\geq\gamma^{thr}_{x_1},a_2|h_{12}|^2\rho_u\geq\gamma^{thr}_{x_{12}})\\&=\begin{cases}1-e^{-\frac{1}{\lambda_{12}}\psi}, & \gamma^{thr}_{x_1}<\frac{a_1}{a_2}\\1, & \gamma^{thr}_{x_1}\geq\frac{a_1}{a_2}\end{cases}\end{aligned} \tag{17}$$

where $\psi=\max(\frac{\gamma^{thr}_{x_1}}{a_1\rho_u-a_2\rho_u\gamma^{thr}_{x_1}},\frac{\gamma^{thr}_{x_{12}}}{a_2\rho_u})$.

Following similar lines as for x_{12}, $P^{out}_{x_{21}}$, $P^{p}_{x_{21}}$ can be calculated from (16), (17) as soon as we replace $\gamma^{thr}_{x_1}$ with $\gamma^{thr}_{x_2}$, $\gamma^{thr}_{x_{12}}$ with $\gamma^{thr}_{x_{21}}$, k_{12} with k_{21}, a_1 and a_2 with b_1 and b_2 respectively.

IV. Ergodic Capacity Analysis

Consider each user's target data rate is dynamically changed depending on user's channel conditions, EC becomes an appropriate performance metric. Since the achievable rate of DF transmission is limited by the weakest link, relay will always forward x^I_r. Moreover, because of the fact that U_2 must decode x_1 before obtains x_{12} in phase-1, the achievable rate for x_1 is $C_{x_1}=\frac{1}{3}\log_2(1+\min(\gamma_{x_1,2},\gamma_{x_1,r},\gamma^{I}_{x_1,b}))$. In a similar manner, for x_2 it holds that $C_{x_2}=\frac{1}{3}\log_2(1+\min(\gamma_{x_2,1},\gamma_{x_2,r},\gamma^{I}_{x_2,b}))$, while the achievable rates for the D2D messages are given as $C_{x_j}=\frac{1}{3}\log_2(1+\gamma_{x_j})$, where $j\in\{12,21\}$. ECs can be calculated by averaging the achievable rates, i.e., $\bar{C}_m=\mathbb{E}\{C_m\}$, where $\mathbb{E}\{\cdot\}$ denotes expectation.

Next, the EC for each data stream will be calculated. For x_1, it holds that $\bar{C}_{x_1}=\mathbb{E}\{\frac{1}{3}\log_2(1+Z)\}$, where $Z=\min(\gamma_{x_1,2},\gamma_{x_1,r},\gamma^{I}_{x_1,b})$. The CDF of Z is calculated by

$$\begin{aligned}F_Z(z)&=1-[1-F_{\gamma_{x_1,2}}(z)][1-F_{\gamma_{x_1,r}}(z)][1-F_{\gamma^{I}_{x_1,b}}(z)]\\&=\begin{cases}1-e^{-\frac{z}{a_1-a_2z}(\frac{1}{\lambda_{1r}\rho_u}+\frac{1}{\lambda_{12}\rho_u}+\frac{1}{\lambda_{rb}\rho_r})}, & z<\frac{a_1}{a_2}\\1, & \text{elsewhere.}\end{cases}\end{aligned} \tag{18}$$

$$P_{x_2}^{out}=\begin{cases}1-e^{-M(b_1,\lambda_{2r},\rho_u,\gamma_{x_2}^{thr})}(e^{-\frac{\gamma_{x_2}^{thr}}{\lambda_{rb}\rho_r}}-e^{-M(a_1,\lambda_{1r},\rho_u,\gamma_{x_1}^{thr})}(-e^{-\frac{\gamma_{x_2}^{thr}}{\lambda_{rb}\rho_r}} & \\ +e^{-\frac{A}{\lambda_{rb}}}(1-e^{-\frac{C}{k_{rb}\lambda_{rb}}})+\frac{1}{Dk_{rb}\lambda_{rb}}e^{-\frac{\gamma_{x_2}^{thr}}{a_2\rho_r\lambda_{rb}}-DC})), & \gamma_{x_1}^{thr}<\frac{a_1}{a_2}, C>0, \gamma_{x_2}^{thr}<\frac{b_1}{b_2} \\ 1-e^{-M(b_1,\lambda_{2r},\rho_u,\gamma_{x_2}^{thr})}(e^{-\frac{\gamma_{x_2}^{thr}}{\lambda_{rb}\rho_r}}-e^{-M(a_1,\lambda_{1r},\rho_u,\gamma_{x_1}^{thr})}(e^{-\frac{\gamma_{x_2}^{thr}}{\lambda_{rb}\rho_r}}-\frac{1}{Dk_{rb}\lambda_{rb}}e^{-\frac{\gamma_{x_2}^{thr}}{a_2\rho_r\lambda_{rb}}})), & \gamma_{x_1}^{thr}<\frac{a_1}{a_2}, C<0, \gamma_{x_2}^{thr}<\frac{b_1}{b_2} \\ 1-e^{-\frac{\gamma_{x_2}^{thr}}{\lambda_{rb}\rho_r}-M(b_1,\lambda_{2r},\rho_u,\gamma_{x_2}^{thr})}, & \gamma_{x_1}^{thr}>\frac{a_1}{a_2}, \gamma_{x_2}^{thr}<\frac{b_1}{b_2} \\ 1, & \text{elsewhere.}\end{cases} \quad (13)$$

By using [11, Eq. (28)], invoking $F_Z(z)$, changing variable of $\frac{z}{a_1-a_2z}=x$, applying partial fraction decomposition and using [13, Eq. (3.352.4)], $\bar{C}_{x_1}$ becomes

$$\begin{aligned}\bar{C}_{x_1}=&-\frac{1}{3\ln 2}\Big\{\mathrm{E_i}(-\frac{1}{\rho_u}(\frac{1}{\lambda_{1r}}+\frac{1}{\lambda_{12}})-\frac{1}{\rho_r\lambda_{rb}})\\ &\times e^{(\frac{1}{\rho_u}(\frac{1}{\lambda_{1r}}+\frac{1}{\lambda_{12}})+\frac{1}{\rho_r\lambda_{rb}})}-\mathrm{E_i}(-\frac{1}{a_2\rho_u}(\frac{1}{\lambda_{1r}}+\frac{1}{\lambda_{12}})\\ &-\frac{1}{a_2\rho_r\lambda_{rb}})\times e^{(\frac{1}{a_2\rho_u}(\frac{1}{\lambda_{1r}}+\frac{1}{\lambda_{12}})+\frac{1}{a_2\rho_r\lambda_{rb}})}\Big\},\end{aligned} \quad (19)$$

where $\mathrm{E_i}(x)=\int_{-\infty}^{x}\frac{e^t}{t}dt,\ x<0$, is the exponential integral function. Similarly with its OP, x_1's EC is not affected from impSIC.

For x_{12}, it holds

$$\bar{C}_{x_{12}}=\mathbb{E}\{\frac{1}{3}\log_2(1+\Gamma)\}=\int_0^{\infty}\frac{1}{3}\log_2(1+\gamma)f_{\Gamma}(\gamma)\mathrm{d}\gamma, \quad (20)$$

where $\Gamma=\gamma_{x_{12}}$. The CDF of Γ is given by $F_{\Gamma}(\gamma)=\Pr(\frac{a_2|h_{12}|^2\rho_u}{a_1|g_{12}|^2\rho_u+1}<\gamma)=1-\frac{a_2\rho_u\lambda_{12}}{a_2\rho_u\lambda_{12}+\gamma a_1\rho_u k_{12}\lambda_{12}}e^{-\frac{\gamma}{a_2\rho_u\lambda_{12}}}$. By letting $\tilde{K}=a_2\rho_u\lambda_{12}$, $\tilde{L}=a_1\rho_u k_{12}\lambda_{12}$, using $\int_0^{\infty}\log_2(1+\gamma)f_{\Gamma}(\gamma)d\gamma=\frac{1}{\ln 2}\int_0^{\infty}\frac{1-F_{\Gamma}(\gamma)}{1+\gamma}d\gamma$ and invoking [13, Eq. (3.352.4)], we get

$$\bar{C}_{x_{12}}=\frac{1}{3\ln 2}\Big\{\frac{\tilde{K}}{\tilde{K}-\tilde{L}}\Big(e^{\frac{1}{\tilde{L}}}E_i(-\frac{1}{\tilde{L}})-e^{\frac{1}{\tilde{K}}}E_i(-\frac{1}{\tilde{K}})\Big)\Big\}. \quad (21)$$

Following similar steps, the EC of x_{21}, can be obtained from (21), as soon as $\tilde{K}$ is replaced with $\bar{K}=b_2\rho_u\lambda_{12}$ and $\tilde{L}$ is replaced with $\bar{L}=b_1\rho_u k_{21}\lambda_{12}$.

On the other hand, if pSIC is considered, then x_{12}'s EC is given as $\bar{C}^p_{x_{12}}=\frac{1}{3\ln 2}\int_0^{\infty}\frac{1-F_{\tilde{\Gamma}}(\gamma)}{1+\gamma}d\gamma$, where $\tilde{\Gamma}=a_2|h_{12}|^2\rho_u$ and $F_{\tilde{\Gamma}}(\gamma)=1-e^{-\frac{\gamma}{\lambda_{12}a_2\rho_u}}$. Hence, invoking [13, Eq. (3.352.4)], it holds $\bar{C}^p_{x_{12}}=-\frac{1}{3\ln 2}e^{\frac{1}{\lambda_{12}a_2\rho_u}}\,\mathrm{E_i}(-\frac{1}{\lambda_{12}a_2\rho_u})$. Similarly, $\bar{C}^p_{x_{21}}=-\frac{1}{3\ln 2}e^{\frac{1}{\lambda_{12}b_2\rho_u}}\,\mathrm{E_i}(-\frac{1}{\lambda_{12}b_2\rho_u})$.

The EC of x_2 is given by $\bar{C}_{x_2}=\mathbb{E}\{\frac{1}{3}\log_2(1+W)\}$, where $W=\min(\gamma_{x_2,1},\gamma_{x_2,r},\gamma^I_{x_2,b})$. The CDFs of $\gamma_{x_2,1}$, $\gamma_{x_2,r}$ can be straightforwardly calculated via (8) and the CDF of $\gamma^I_{x_2,b}$ can be given as $F_{\gamma^I_{x_2,b}}(x)=\Pr(\frac{a_2|h_{rb}|^2\rho_r}{a_1|g_{rb}|^2\rho_r+1}<x)=1-\frac{a_2\lambda_{rb}\rho_r}{\lambda_{rb}k_{rb}a_1\rho_r x+a_2\lambda_{rb}\rho_r}e^{-\frac{x}{a_2\lambda_{rb}\rho_r}}$. Hence, the CDF of W is

$$F_W(w)=\begin{cases}1-\frac{a_2\lambda_{rb}\rho_r}{\lambda_{rb}k_{rb}a_1\rho_r x+a_2\lambda_{rb}\rho_r}e^{-\frac{w}{\lambda_{rb}a_2\rho_r}} & \\ \quad\times e^{-\frac{w}{b_1-b_2w}(\frac{1}{\lambda_{2r}\rho_u}+\frac{1}{\lambda_{12}\rho_u})}, & w<\frac{b_1}{b_2}\\ 1, & \text{elsewhere.}\end{cases} \quad (22)$$

Hence, by applying $F_W(w)$ in [11, Eq. (28)], it holds

$$\bar{C}_{x_2}=\frac{1}{3\ln 2}\int_0^{\frac{b_1}{b_2}}\frac{1-F_W(w)}{1+w}\mathrm{d}w \quad (23)$$

The integral in (23) cannot be calculated in a closed-form. However, when $\rho_u=\rho_r=\rho\to\infty$, it holds that $W=\min(\frac{b_1}{b_2},\gamma^I_{x_2,b})$. Thus, at high SNR, an approximation (ap.) can be given as

$$\begin{aligned}\bar{C}^{\infty}_{x_2}&=\frac{1}{3}\int_{\frac{b_1}{b_2}}^{\infty}\log_2(1+\frac{b_1}{b_2})f_{\gamma^I_{x_2,b}}(\gamma)\mathrm{d}\gamma+\frac{1}{3}\int_0^{\frac{b_1}{b_2}}\log_2(1+\gamma)\\ &\times f_{\gamma^I_{x_2,b}}(\gamma)\mathrm{d}\gamma=\frac{1}{3\ln 2}\int_0^{\frac{b_1}{b_2}}\frac{1-F_{\gamma^I_{x_2,b}}(\gamma)}{1+\gamma}\mathrm{d}\gamma\\ &=\frac{1}{3\ln 2}\Big\{\frac{K}{K-L}\Big(\int_0^{\frac{b_1}{b_2}}\frac{e^{-\frac{\gamma}{K}}}{(1+\gamma)}\mathrm{d}\gamma-\int_0^{\frac{b_1}{b_2}}\frac{L}{K+L\gamma}e^{-\frac{\gamma}{K}}\mathrm{d}\gamma\Big)\Big\}\\ &\overset{(b)}{=}\frac{1}{3\ln 2}\Big\{\frac{K}{K-L}\Big[e^{\frac{1}{K}}\Big(E_i(-\frac{1}{K}\frac{b_1}{b_2}-\frac{1}{K})-E_i(-\frac{1}{K})\Big)\\ &\quad-e^{\frac{1}{L}}\Big(E_i(-\frac{1}{K}\frac{b_1}{b_2}-\frac{1}{L})-E_i(-\frac{1}{L})\Big)\Big]\Big\},\end{aligned} \quad (24)$$

where (b) comes from invoking [13, Eq. (3.352.1)] and $L=\lambda_{rb}k_{rb}a_1\rho_r$, $K=a_2\lambda_{rb}\rho_r$.

In case of pSIC, x_2's EC, denoted as $\bar{C}^p_{x_2}$, can be given from (23) as soon as W is replaced with $\tilde{W}=\min(\gamma_{x_2,1},\gamma_{x_2,r},a_2|h_{rb}|^2\rho_r)$, where

$$F_{\tilde{W}}(\tilde{w})=\begin{cases}1-e^{-\frac{\tilde{w}}{b_1-b_2\tilde{w}}(\frac{1}{\lambda_{2r}\rho_u}+\frac{1}{\lambda_{12}\rho_u})-\frac{\tilde{w}}{\lambda_{rb}a_2\rho_r}}, & \tilde{w}<\frac{b_1}{b_2}\\ 1, & \text{elsewhere.}\end{cases} \quad (25)$$

However, the above integral cannot be calculated in closed-form. Nonetheless, when $\rho\to\infty$, it holds that $\tilde{W}=\min(\frac{b_1}{b_2},a_2|h_{rb}|^2\rho_r)$. Thus, following similar lines with the extraction of (24), at high SNR, it holds

$$\bar{C}^{p,\infty}_{x_2}=\frac{e^{\frac{1}{a_2\rho_r\lambda_{rb}}}}{3\ln 2}\Big(\mathrm{E_i}(-\frac{1}{a_2\rho_r\lambda_{rb}}(1+\frac{b_1}{b_2}))-\mathrm{E_i}(-\frac{1}{a_2\rho_r\lambda_{rb}})\Big). \quad (26)$$

A. Ergodic Sum Capacity

The ESC of the proposed scheme, under pSIC and impSIC, can be calculated as $\bar{C}^p_{sum}=\bar{C}_{x_1}+\bar{C}^p_{x_2}+\bar{C}^p_{x_{12}}+\bar{C}^p_{x_{21}}$ and $\bar{C}_{sum}=\bar{C}_{x_1}+\bar{C}_{x_2}+\bar{C}_{x_{12}}+\bar{C}_{x_{21}}$, respectively.

A theorem that investigates the performance of ESC at the high-SNR regime follows.

Theorem 1. *When $\rho\to\infty$, $\bar{C}^p_{sum}$ scales as $\frac{2}{3}\log_2(\rho)$.*

Proof: By replacing $\mathrm{E_i}(x)_{x\to 0}\sim C+\ln(-x)+x$, where C denotes the Euler constant, and $e^{-x}_{x\to 0}\sim 1-x$ in $\bar{C}_{x_1}$, $\bar{C}^p_{x_2}$, $\bar{C}^p_{x_{12}}$, $\bar{C}^p_{x_{21}}$ and performing straightforward algebraic manipulations, it can be shown that $\bar{C}^p_{sum}\sim\frac{2}{3}\log_2(\rho)$. ■

V. Numerical Results and Discussion

In this section, both simulations (sim.) and analytical results for BD2D-CNOMA are presented. A fixed power allocation method is assumed [7], [11], thus, we set $a_1=0.7$, $b_1=0.75$.

This article has been accepted for publication in IEEE Communications Letters. This is the author's version which has not been fully edited and
content may change prior to final publication. Citation information: DOI 10.1109/LCOMM.2022.3199083

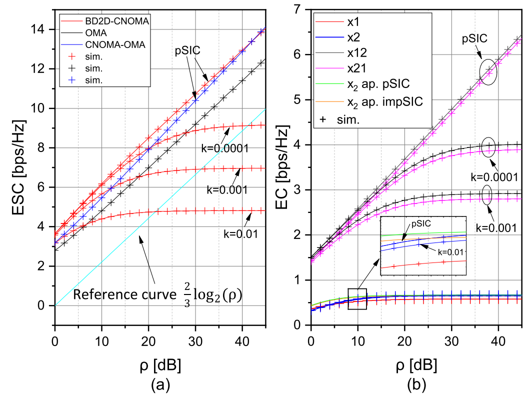

Fig. 2: E(S)C comparisons vs ρ: (a) between BD2D-CNOMA and benchmarks, (b) among users in BD2D-CNOMA.

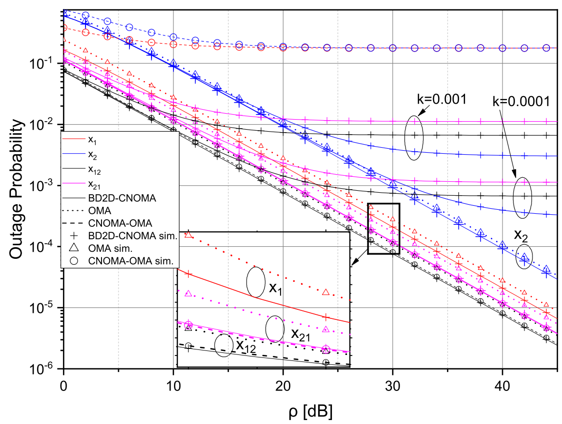

Fig. 3: Users' OPs vs ρ for BD2D-CNOMA and benchmarks.

Without loss of generality, similarly with [7], we consider the normalized distances $d_{U_2,r}+d_{r,BS}=1$, $d_{r,BS}=0.5$, $d_{U_1,r}=0.3$, $d_{U_1,U_2}=0.2$, $d_{U_2,r}=0.5$. Also, it is assumed that $\rho_u=\rho_r=\rho$, $\epsilon=3$ and $k_{12}=k_{21}=k_{rb}=k$. As benchmarks, an OMA scheme and a hybrid CNOMA-OMA scheme with pSIC are considered. OMA with time division multiple access requires six time slots to transmit all messages. CNOMA-OMA requires 4 time slots: 1) U_1, U_2 simultaneously transmit x_1, x_2 to the relay which decodes the messages with order (x_1,x_2), 2) relay forwards $x_r=\sqrt{a_1P_r}x_1+\sqrt{a_2P_r}x_2$ to BS, 3) U_1 transmits x_{12} to U_2, 4) U_2 transmits x_{21} to U_1.

In Fig. 2-(a), ESC comparison between BD2D-CNOMA and benchmarks is presented versus ρ, while in Fig. 2-(b) users' ECs for BD2D-CNOMA are provided versus ρ. Analytical values coincide with simulation results, thus verifying the presented analysis. In Fig. 2-(a), proposed scheme's ESC under pSIC scales as $\frac{2}{3}\log_2(\rho)$, as predicted by Theorem 1. Furthermore, it is obvious that under pSIC, compared to benchmarks, BD2D-CNOMA achieves higher ESC for almost every ρ. Under impSIC, ESC shows an initial increase, which is followed by a ceiling value. This happens because of the residual interference caused by impSIC. As parameter k increases, the ceiling values become lower. In Fig. 2-(b), it is illustrated that, under pSIC, x_{12}'s, x_{21}'s ECs keep increasing with respect to ρ, whereas, under impSIC, ECs converge to a ceiling. Moreover, ECs of x_1, x_2 increase up to a ρ value and then remain flat. Also, it is evident that x_2's EC, compared to ECs of x_{12}, x_{21}, is not greatly affected from impSIC; this happens since the only term of W affected from impSIC is $\gamma^I_{x_1,b}$, which is generally greater than $\gamma_{x_2,1}$, $\gamma_{x_2,r}$ and, thus, does not significantly affect the min operator in W.

Fig. 3 illustrates users' OPs for BD2D-CNOMA and benchmarks versus ρ. Target rates $\bar{R}_1=0.25$, $\bar{R}_2=0.4$, $\bar{R}_{12}=0.65$, $\bar{R}_{21}=0.75$ were assumed. Compared to OMA, it is illustrated that, under pSIC, BD2D-CNOMA leads to improved OPs for all messages. Compared to CNOMA-OMA and under pSIC, in BD2D-CNOMA no OP floors appear for the cellular messages, while the two schemes achieve similar performances for the D2D messages. Under impSIC, except x_1's OP, the OPs of all messages reach floors at high-SNR due to the residual interference. The increase of k leads to decrease of the floor values. Also, although under pSIC x_2 shows the worst outage behavior, under impSIC x_2's floor is lower than x_{12}'s, x_{21}'s floors; this is expected since impSIC affects only one of the terms that appear in (10), whereas the only term that appears in the extraction of x_{12}'s, x_{21}'s OP is significantly affected from impSIC.

VI. Conclusion

The proposed BD2D-CNOMA shows that cellular and bidirectional D2D communications can occur simultaneously in the same frequency, achieving enhanced SE. The performance of the proposed scheme is investigated in terms of EC, ESC and OP under both pSIC and impSIC. Simulation results manifest its superiority over conventional benchmarks under pSIC and illustrate useful insights for the case of impSIC.

References

[1] Z. Ding, X. Lei, G. K. Karagiannidis, R. Schober, J. Yuan, and V. K. Bhargava, "A survey on non-orthogonal multiple access for 5G networks: Research challenges and future trends," *IEEE J. Sel. Areas Commun.*, vol. 35, no. 10, pp. 2181–2195, 2017.

[2] Z. Ding, M. Peng, and H. V. Poor, "Cooperative non-orthogonal multiple access in 5G systems," *IEEE Commun. Lett.*, vol. 19, no. 8, pp. 1462–1465, 2015.

[3] F. Jameel, Z. Hamid, F. Jabeen, S. Zeadally, and M. A. Javed, "A survey of Device-to-Device communications: Research issues and challenges," *IEEE Commun. Surveys Tuts.*, vol. 20, no. 3, pp. 2133–2168, 2018.

[4] Z. Zhang, Z. Ma, M. Xiao, Z. Ding, and P. Fan, "Full-duplex Device-to-Device-aided cooperative non-orthogonal multiple access," *IEEE Trans. Veh. Technol.*, vol. 66, no. 5, pp. 4467–4471, 2016.

[5] Q. Y. Liau and C. Y. Leow, "Successive user relaying in cooperative NOMA system," *IEEE Wireless Commun. Lett.*, vol. 8, no. 3, pp. 921–924, 2019.

[6] J. Liu, G. Wu, S. Xiao, X. Zhou, G. Y. Li, S. Guo, and S. Li, "Joint power allocation and user scheduling for Device-to-Device-enabled heterogeneous networks with non-orthogonal multiple access," *IEEE Access*, vol. 7, pp. 62 657–62 671, 2019.

[7] L. Zou, J. Chen, L. Lv, and B. He, "Capacity enhancement of D2D aided coordinated direct and relay transmission using NOMA," *IEEE Commun. Lett.*, vol. 24, no. 10, pp. 2128–2132, 2020.

[8] J.-B. Kim, I.-H. Lee, and J. Lee, "Capacity scaling for D2D aided cooperative relaying systems using NOMA," *IEEE Wireless Commun. Lett.*, vol. 7, no. 1, pp. 42–45, 2017.

[9] Y. Xu, B. Li, N. Zhao, Y. Chen, G. Wang, Z. Ding, and X. Wang, "Coordinated direct and relay transmission with NOMA and network coding in Nakagami-m fading channels," *IEEE Trans. Commun.*, vol. 69, no. 1, pp. 207–222, 2020.

[10] M. F. Kader, S. R. Islam, and O. A. Dobre, "Simultaneous cellular and D2D communications exploiting cooperative uplink NOMA," *IEEE Commun. Lett.*, vol. 25, no. 6, pp. 1848–1852, 2021.

[11] Y. Zhang, S. Feng, and W. Tang, "Performance analysis of hybrid cellular and bidirectional Device-to-Device cooperative NOMA communication systems," *IEEE Trans. Veh. Technol.*, vol. 70, no. 10, pp. 10 420–10 435, 2021.

[12] Q. Ye, M. Al-Shalash, C. Caramanis, and J. G. Andrews, "Distributed resource allocation in Device-to-Device enhanced cellular networks," *IEEE Trans. Commun.*, vol. 63, no. 2, pp. 441–454, 2014.

[13] I. S. Gradshteyn and I. M. Ryzhik, *Table of integrals, series, and products*. Academic press, 2014.